

Quantum Field Theory of Graphene with Dynamical Partial Symmetry Breaking

Halina V. Grushevskaya, George Krylov

Physics Department, Belarusian State University, Minsk, Belarus
Email: grushevskaja@bsu.by

Received 17 April 2014; revised 14 May 2014; accepted 11 June 2014

Copyright © 2014 by authors and Scientific Research Publishing Inc.
This work is licensed under the Creative Commons Attribution International License (CC BY).
<http://creativecommons.org/licenses/by/4.0/>



Open Access

Abstract

The quantum field theory approach has been proposed for the description of graphene electronic properties. It generalizes massless Dirac fermion model and is based on the Dirac-Hartree-Fock self-consistent field approximation and assumption on antiferromagnetic ordering of graphene lattice. The developed approach allows asymmetric charged carriers in single layer graphene with partially degenerated Dirac cones.

Keywords

Graphene, Asymmetric Charged Carriers, Dirac-Hartree-Fock Self-Consistent Field Approximation

1. Introduction

The ongoing boom in experimental researches of graphene is not accompanied, however, by substantial development of nanoelectronic components using its unique properties. The one of the possible reasons of this situation could be the absence of satisfactory description of its electrophysical properties on the basis of quantum field theory.

The *ab initio* calculations by muffin-tin orbital method and usage of random phase approximation (RPA) for polarization operator to investigate the balance of exchange and correlation interactions on band structure of loosely-packed crystals have shown that strong exchange leads to appearance of an energy gap in the spectrum [1]. Conversely, strong correlation interaction leads to tightening the gap in the band spectrum. The spin non-polarized *ab initio* simulations of partial electron densities of two-dimensional graphite have shown that the material is a semiconductor. Interlayer correlations tighten energy gap that results in semi-metal behaviour of three-dimensional graphite [1]. The presence of a gap in band spectrum of graphene (at Dirac points K, K') would increase theoretical estimation of its conductivity to $\pi e^2/h$ that is to value approaching optical (high frequency) conductivity of graphene [1]. But there is a significant discrepancy of theoretical estimates of low-frequency

(minimal) conductivity of monolayer graphene [3]-[5] with its experimental value $4e^2/h$ [6]-[12].

Energy gap ~ 10 meV can be in spectra of nanostructures with photon-dressed ground state [13]. With measurement accuracy ~ 1 meV, permissible at the present level of technological development, the gap is not registered [14], though a sharp change of the Fermi velocity v_F in Dirac point $K(K')$, described in Hartree-Fock and RPA [14], as well as when using the *ab initio* simulations [15] is the experimental fact [14].

Quantum field theory [16] of pseudo-Dirac quasiparticles [17]-[20] in RPA gives a strong screening which destroys the excitonic pairing instability if dynamic fermion mass m_q is small in comparison with chemical potential μ : $m_q \leq \mu$. The existence of dynamic screening for this system with physical flavor $N = 2$, calculated by Eliashberg self-consistent technique, makes the value of m_q non-zero for momentums $|q| < 10^{-6}$ [16]. Unfortunately, such a range of values of q also gives practically vanishing mass $m_{k_F} \sim q/v_F < 10^{-12}$ for the Fermi momentum k_F and Fermi velocity $v_F \sim 10^6$ m/s. Additional possible lack of this approach is that though pseudo-Dirac fermions act in $2 + 1$ dimensional space-time, an electromagnetic field is defined as usual in $3 + 1$ dimensions [2] [16] [21] (otherwise Coulomb interaction in 2D space would be $\log r$ rather than needed $1/r$).

In papers [22]-[24] one uses a known analogy between the mass of a particle in the kinetic energy and a factor entered as the mass tensor m^{ij} in a quadratic term in the energy expansion of a single-particle state; the magneto-transport term for which there is no such an analogy is discarded. Such description of particles collisions in impurity-free (pure) graphene as electron-phonon scattering gives an estimate of the dynamic conductivity $\pi e^2/(2h)$ at low temperature $T \rightarrow 0$ [22]-[24].

In the reference frame where a fermion with nonzero rest mass moves with a velocity v , its bispinor wave function $\Psi(t) = \{\Psi_\sigma^{up}(t), \Psi_\sigma^{down}(t)\}$ in addition to non-zero upper components $\Psi_\sigma^{up}(t)$ acquires non-zero lower (“positron”) components $\Psi_\sigma^{down}(t)$ [25] [26]

$$\Psi_\sigma^{up}(t) = \frac{1}{\sqrt{2}}(\cosh \chi + 1)^{1/2} e^{-i\epsilon t} \psi_{p1}, \quad \Psi_\sigma^{down}(t) = \frac{1}{\sqrt{2}} \frac{\boldsymbol{\sigma} \cdot \mathbf{p}}{p} (\cosh \chi - 1)^{1/2} e^{-i\epsilon t} \psi_{p1}, \quad \cosh^{-1} \chi = \sqrt{1 - v^2/c^2}. \quad (1)$$

Changing the light speed $c \rightarrow v_F$ in (1), the pseudo-spinor wave function $\Psi_p(t)$ of quasiparticles in graphene can be written as a sum of electron wave functions (1):

$$\Psi_p(t) = \frac{1}{2} \left[\Psi_\sigma^{up}(t) + \Psi_\sigma^{down}(t) + (\Psi_{-\sigma}^{up}(t) + \Psi_{-\sigma}^{down}(t))^\dagger \right] \sim \frac{1}{2} \left[e^{-i\epsilon_p t} (1 + \boldsymbol{\sigma} \cdot \mathbf{p}/p) + e^{i\epsilon_p t} (1 - \boldsymbol{\sigma} \cdot \mathbf{p}/p) \right] \Psi_p \quad (2)$$

where $\epsilon_p = v_F p/\hbar$. Due to the process of electron-hole pairs’ production, the current \mathbf{j} [27] oscillates [28]

$$\mathbf{j}(t) = \mathbf{j}_0 + \mathbf{j}_1 + \mathbf{j}_1^\dagger, \quad \mathbf{j}_0 = e v_F \sum_p \Psi_p^\dagger \frac{p(\mathbf{p} \cdot \boldsymbol{\sigma})}{p^2} \Psi_p, \quad \mathbf{j}_1 = \frac{e v_F}{2} \sum_p \Psi_p^\dagger \left[\boldsymbol{\sigma} - \frac{p(\mathbf{p} \cdot \boldsymbol{\sigma})}{p^2} + \frac{i}{p} \boldsymbol{\sigma} \times \mathbf{p} \right] \Psi_p e^{2i\epsilon_p t} \quad (3)$$

where oscillating summands $\mathbf{j}_1, \mathbf{j}_1^\dagger$ are called “Zitterbewegung” terms. Drawback of pseudo-electrodynamics of graphene [28] is the divergence of the expression (2) at $v \rightarrow v_F$.

Weak localization of states can be introduced through non-zero spin-orbit interaction. A possibility of the absence of inversion center for spin-polarized electron density of monolayer grapheme, related with this fact possibility of non-zero spin-orbit contribution $H_{SO}^{G,I}$, which depends upon z -component of Pauli matrices vector (spin) and pseudo-Pauli matrices vector (pseudo-spin) and stipulates magnetoelectric effects, has been mentioned in papers [29]-[31]. The phenomenon of spin dependent scattering in non-magnetic graphene can be viewed as an experimentally proven charged carrier asymmetry in graphene [32] [33]. Intrinsic and extrinsic (Rashba) spin-orbit couplings in single layer graphene manifest themselves via the Elliot-Yafet and Dyakonov-Perel disorder-scattering spin-relaxation mechanisms, respectively [34]. The development of quantum spintronic devices is based on spin-dependent bands simulations. These simulations demonstrate that intrinsic spin-orbital interaction is very small, less than 100 μeV [35]. Resonant mechanism of the skew scattering, stipulated by increase of the strength of spin-orbital coupling up to ~ 10 meV in the presence of a metal cluster, has been proposed in [36]. Despite the fact that the non-equilibrium spin can occur in a resonantly acting field (plasmons) of metal cluster near the surface of graphene (the Hanle effect), the presence of such an impurity is also accompanied by the removal of degeneracy of the Dirac cone. The last one leads to the appearance of a hexagon of mini-zones in the vicinity of Dirac cone; respectively, electron-hole asymmetry has another origin which is not related with spin-orbital interaction. In [2] [3] [13] [37], the conductivity of graphene has been de-

scribed via the appearance of a gap stipulated by excitonic pairing mechanism and with a value of the same order of magnitude as the aforementioned (induced) one. Besides, the Hall effect is accompanied by intensive process of electron-hole symmetric pair production in the form of “Zitterbewegung” for wave functions [3] [27] [37]. This demonstrates that the “Zitterbewegung” phenomena and the gap of nanostructures with photon-dressed ground states are capable to neutralize resonant mechanism of the induced skew symmetry.

Electromagnetic interaction between N Dirac particles leads to a renormalization of their masses [38]. On the one hand, this dynamic (renormalized) mass m_q of charged carriers in graphene should be sufficiently small: $m_q \leq \mu$, to be an agreement with experimental data. On the other hand, the value of m_q should be finite that allows at least getting a match with the experimental value of the dynamic conductivity of graphene [2] [22].

The most promising is the use of Dirac-Hartree-Fock self-consistent field approximation for the description of spin-dependent electrical properties of graphene, since the estimate of dynamic mass of the quasiparticles in graphene in this approximation is given by $\overline{\Sigma_{AB}\Sigma_{BA}}/c \sim 10^{-8}$ [39].

Charged carrier asymmetry in graphene transport experimentally found in [40] [41] by a method [42], allows assuming non-coincidence of Dirac cone with its replica except for $K(K')$ -point. In the paper [43], it has been shown that in the flavor model $N = 2$ charged carriers are symmetric as well as the graphene band structure.

The goal of this paper is to construct a pseudo-bispinor description of graphene, which is based on the Dirac-Hartree-Fock self-consistent field approximation, and to propose a flavor model $N = 3$ for the graphene with spin-polarized sublattices. Coulomb interaction in the model is dynamically screened not due to self-consistent motion of an electron with respect to a hole as in flavor models $N = 2$, but due to self-consistent motion of negatively charged three-particle exciton state relative to positively charged three-particle exciton ($N = 3$).

The paper is organized as follows. In Sections 2 and 3 we shortly introduce the approach [39] and use it in a simple tight-binding approximation of the problem and massless case. Section 4 gives explicit expressions for exchange interaction matrices allowing further simulating quantities of interest, which are performed and discussed in Sections 5 and 6; in Section 7 we summarize our findings.

2. The Equations of Self-Consistent Charged Carriers Motion in Graphene

In papers [39] [44]-[46] a new approach has been proposed to describe graphene electronic properties. It utilizes a quasi-relativistic Dirac-Hartree-Fock self-consistent field approximation and assumption on ferromagnetic ordering of the sublattices A, B (with anti-ferromagnetic ordering of the lattice as a whole). In this approach the graphene is described by the following stationary equation for the second-quantized fermion field $\hat{\chi}_{-\sigma_A}^\dagger$:

$$\left\{ \boldsymbol{\sigma} \cdot \mathbf{p} \hat{v}_F^{qu} - (1/c) \left(i \Sigma_{rel}^x \right)_{AB} \left(i \Sigma_{rel}^x \right)_{BA} \right\} \hat{\chi}_{-\sigma_A}^\dagger(\mathbf{r}) |0, -\sigma\rangle = E_{qu}(p) \hat{\chi}_{-\sigma_A}^\dagger(\mathbf{r}) |0, -\sigma\rangle. \quad (4)$$

Here points $K(K')$ in the Brillouin zone of monolayer graphene are designated as $K_A(K_B)$, \mathbf{p} is the momentum operator, operator \hat{v}_F^{qu} is defined as

$$\hat{v}_F^{qu} = \left[\left(\Sigma_{rel}^x \right)_{BA} + c \hbar \boldsymbol{\sigma} \cdot (\mathbf{K}_A + \mathbf{K}_B) \right]. \quad (5)$$

$\boldsymbol{\sigma} = (\sigma_x, \sigma_y, \sigma_z)$ is the vector of Pauli matrices, 2D transformation matrices $\left(\Sigma_{rel}^x \right)_{BA}, \left(\Sigma_{rel}^x \right)_{AB}$ are determined by an exchange interaction term Σ_{rel}^x

$$\Sigma_{rel}^x \begin{pmatrix} \hat{\chi}_{-\sigma_A}^\dagger(\mathbf{r}) \\ \hat{\chi}_{-\sigma_B}^\dagger(\mathbf{r}) \end{pmatrix} |0, -\sigma\rangle |0, \sigma\rangle = \begin{pmatrix} 0 & \left(\Sigma_{rel}^x \right)_{AB} \\ \left(\Sigma_{rel}^x \right)_{BA} & 0 \end{pmatrix} \begin{pmatrix} \hat{\chi}_{-\sigma_A}^\dagger(\mathbf{r}) \\ \hat{\chi}_{-\sigma_B}^\dagger(\mathbf{r}) \end{pmatrix} |0, -\sigma\rangle |0, \sigma\rangle, \quad (6)$$

$$\left(\Sigma_{rel}^x \right)_{AB} \hat{\chi}_{\sigma_B}^\dagger(\mathbf{r}) |0, \sigma\rangle = \sum_{i=1}^{NN_y} \int d\mathbf{r}_i \hat{\chi}_{\sigma_i^B}^\dagger(\mathbf{r}_i) |0, \sigma\rangle \langle 0, -\sigma_i | \hat{\chi}_{-\sigma_i^A}^\dagger(\mathbf{r}_i) V(\mathbf{r}_i - \mathbf{r}) \hat{\chi}_{-\sigma_B}(\mathbf{r}_i) |0, -\sigma_i\rangle, \quad (7)$$

$$\left(\Sigma_{rel}^x \right)_{BA} \hat{\chi}_{-\sigma_A}^\dagger(\mathbf{r}) |0, -\sigma\rangle = \sum_{i'=1}^{NN_y} \int d\mathbf{r}_{i'} \hat{\chi}_{-\sigma_{i'}^A}^\dagger(\mathbf{r}_{i'}) |0, -\sigma\rangle \langle 0, \sigma_{i'} | \hat{\chi}_{\sigma_{i'}^B}^\dagger(\mathbf{r}_{i'}) V(\vec{r}_{i'} - \vec{r}) \hat{\chi}_{\sigma_A}(\mathbf{r}_{i'}) |0, \sigma_{i'}\rangle. \quad (8)$$

Now, we perform the following non-unitary transformation of the wave function for graphene

$$\widehat{\tilde{\chi}}_{-\sigma_A}^\dagger |0, -\sigma\rangle = \left(\Sigma_{rel}^x \right)_{BA} \widehat{\chi}_{-\sigma_A}^\dagger |0, -\sigma\rangle. \quad (9)$$

In the limit of $|q| \ll 1$ we can neglect the mixing of the states for the Dirac points K_A and K_B , and get

pure two-dimensional case. After this transformation, Equation (4) takes the form similar to a pseudo-Dirac approximation of two-dimensional graphene:

$$\{c\sigma_{2D}^{AB} \cdot \mathbf{p}_{BA} - \widetilde{\Sigma_{BA}\Sigma_{AB}}\} \hat{\chi}_{-\sigma_A}^\dagger(\mathbf{r})|0, -\sigma\rangle = c\tilde{E}_{qu}(p) \hat{\chi}_{-\sigma_A}^\dagger(\mathbf{r})|0, -\sigma\rangle, \quad q \ll 1 \quad (10)$$

where $\widetilde{\Sigma_{BA}\Sigma_{AB}} = -(\Sigma_{rel}^x)_{BA} (\Sigma_{rel}^x)_{AB}$, $\sigma_{2D}^{AB} = (\Sigma_{rel}^x)_{BA} \sigma_{2D} (\Sigma_{rel}^x)_{BA}^{-1}$, $\sigma_{2D} = (\sigma_x, \sigma_y)$,

$$\mathbf{p}_{BA} \hat{\chi}_{-\sigma_A}^\dagger = (\Sigma_{rel}^x)_{BA} \mathbf{p} (\Sigma_{rel}^x)_{BA}^{-1} \hat{\chi}_{-\sigma_A}^\dagger, \quad \tilde{E}_{qu} = E_{qu} \hat{v}_F^{-1}.$$

In a similar way we can write down the following stationary equation for the second quantized fermion field $\hat{\chi}_{+\sigma_B}^\dagger$ on the sublattice B :

$$\left[c\sigma_{2D}^{BA} \cdot \mathbf{p}_{AB} - \widetilde{\Sigma_{AB}\Sigma_{BA}}(\mathbf{p}) \right] \hat{\chi}_{+\sigma_B}^\dagger(\mathbf{r})|0, \sigma\rangle = c\tilde{E}_{qu}(p) \hat{\chi}_{+\sigma_B}^\dagger(\mathbf{r})|0, \sigma\rangle \quad (11)$$

where $\widetilde{\Sigma_{AB}\Sigma_{BA}} = -(\Sigma_{rel}^x)_{AB} (\Sigma_{rel}^x)_{BA}$, $\mathbf{p}_{AB} = (\Sigma_{rel}^x)_{AB} \mathbf{p} (\Sigma_{rel}^x)_{AB}^{-1}$, $\hat{\chi}_{+\sigma_B}^\dagger(\mathbf{r})|0, \sigma\rangle = (\Sigma_{rel}^x)_{AB} \hat{\chi}_{+\sigma_B}^\dagger(\mathbf{r})|0, \sigma\rangle$.

Due to the fact that $(\Sigma_{rel}^x)_{BA} \neq (\Sigma_{rel}^x)_{AB}$, the vector \mathbf{p}_{BA} of the Dirac cone is somehow rotated and stretched in respect to the vector \mathbf{p}_{AB} of its replica.

3. The Equation of Motion of Massless Charged Carriers in Graphene

Massless approximation of Equation (10) reads

$$\sigma_{2D}^{BA} \cdot \mathbf{p}_{AB} \hat{\chi}_{+\sigma_B}^\dagger(\mathbf{r})|0, -\sigma\rangle = E_{qu}(p) \hat{\chi}_{+\sigma_B}^\dagger(\mathbf{r})|0, -\sigma\rangle. \quad (12)$$

Let wave functions ϕ_\uparrow and ϕ_\downarrow with spin up and down respectively has the form

$$\phi_\uparrow = \frac{1}{\sqrt{2}} \begin{pmatrix} \phi_1 \\ 0 \end{pmatrix}, \quad \phi_\downarrow = \frac{1}{\sqrt{2}} \begin{pmatrix} 0 \\ \phi_2 \end{pmatrix}. \quad (13)$$

Bispinor wave functions of quasiparticles moving on the Dirac cones and its replicas can be represented as the free Dirac field of π (p_z)-electrons:

$$\begin{pmatrix} \hat{\chi}_{-\sigma_{A(B)}}^\dagger(\mathbf{r})|0, -\sigma\rangle \\ \hat{\chi}_{+\sigma_{B(A)}}^\dagger(\mathbf{r})|0, \sigma\rangle \end{pmatrix} = \frac{e^{-i(\mathbf{K}_{A(B)} - \mathbf{q}_{A(B)}) \cdot \mathbf{r}}}{\sqrt{2}} \begin{pmatrix} \exp\{-i\theta_{k_{A(B)}}\} \phi_1 \\ \exp\{-i\theta_{k_{A(B)}}\} \phi_2 \\ -\exp\{i\theta_{k_{B(A)}}\} \phi_2 \\ \exp\{i\theta_{k_{B(A)}}\} \phi_1 \end{pmatrix} \equiv \begin{pmatrix} \chi_{-\sigma_{A(B)}} \\ \chi_{+\sigma_{B(A)}} \end{pmatrix}, \quad (14)$$

$$\begin{pmatrix} \widehat{\chi}_{+\sigma_{A(B)}}^\dagger(\mathbf{r})|0, \sigma\rangle \\ \widehat{\chi}_{-\sigma_{B(A)}}^\dagger(\mathbf{r})|0, -\sigma\rangle \end{pmatrix} = \frac{e^{-i(\mathbf{K}_{A(B)} - \mathbf{q}_{A(B)}) \cdot \mathbf{r}}}{\sqrt{2}} \begin{pmatrix} -\exp\{i\theta_{k_{A(B)}}\} \phi_2 \\ \exp\{i\theta_{k_{A(B)}}\} \phi_1 \\ \exp\{-i\theta_{k_{B(A)}}\} \phi_1 \\ \exp\{-i\theta_{k_{B(A)}}\} \phi_2 \end{pmatrix} \equiv \begin{pmatrix} \chi_{+\sigma_{A(B)}} \\ \chi_{-\sigma_{B(A)}} \end{pmatrix} \quad (15)$$

where

$$\phi_i = \frac{1}{(2\pi)^{3/2} \sqrt{N/2}} \sum_{\mathbf{R}_i^{A(B)}} \exp\{i[\mathbf{K}_{A(B)} - \mathbf{q}_{A(B)}][\mathbf{R}_i^{A(B)} - \mathbf{r}]\} \psi_{\{n_i\}}(\mathbf{r} - \mathbf{R}_i^{A(B)}) \quad (16)$$

is a Bloch function.

In approximation of free π (p_z)-electrons all wave functions entering into the expressions (7), (8) are de-

scribed by the Formulae (14), (15):

$$\hat{\chi}_{-\sigma_A}^\dagger(\mathbf{r}) \equiv \widehat{\chi_{-\sigma_A}^\dagger}(\mathbf{r}), \quad \hat{\chi}_{\sigma_B}^\dagger(\mathbf{r}) \equiv \widehat{\chi_{\sigma_B}^\dagger}(\mathbf{r}) \quad \text{for } \forall i, i'. \quad (17)$$

Then, in this approximation we can write matrices $(\Sigma_{rel}^x)_{AB} \approx \Sigma_{AB}$ and $(\Sigma_{rel}^x)_{BA} \approx \Sigma_{BA}$ without self-action as

$$\begin{aligned} (\Sigma_{rel}^x)_{AB} \widehat{\chi_{+\sigma_B}^\dagger}(\mathbf{r})|0, \sigma\rangle &\approx \Sigma_{AB} \chi_{\sigma_B} = \sum_{i=1}^{N_i N-1} \int d\mathbf{r}_i V(\mathbf{r}_i - \mathbf{r}) [\chi_{-\sigma_A}(\mathbf{r}_i) \cdot \chi_{-\sigma_B}^*(\mathbf{r}_i)] \chi_{+\sigma_B}(\mathbf{r}) \\ &= \frac{1}{2^{3/2}} \sum_{i=1}^{N_i N-1} \int d\mathbf{r}_i V(\mathbf{r}_i - \mathbf{r}) \begin{bmatrix} e^{-i\theta_{k_A}} \phi_1(\mathbf{r}_i) e^{i\theta_{k_B}} \phi_1^*(\mathbf{r}_i) & e^{-i\theta_{k_A}} \phi_1(\mathbf{r}_i) e^{i\theta_{k_B}} \phi_2^*(\mathbf{r}_i) \\ e^{-i\theta_{k_A}} \phi_2(\mathbf{r}_i) e^{i\theta_{k_B}} \phi_1^*(\mathbf{r}_i) & e^{-i\theta_{k_A}} \phi_2(\mathbf{r}_i) e^{i\theta_{k_B}} \phi_2^*(\mathbf{r}_i) \end{bmatrix} \begin{bmatrix} e^{-i[(K_A - q_A)\mathbf{r} - \theta_{k_B}]} \phi_2(\mathbf{r}) \\ e^{-i[(K_A - q_A)\mathbf{r} - \theta_{k_B}]} \phi_1(\mathbf{r}) \end{bmatrix}, \end{aligned} \quad (18)$$

$$\begin{aligned} (\Sigma_{rel}^x)_{BA} \widehat{\chi_{-\sigma_A}^\dagger}(\mathbf{r})|0, -\sigma\rangle &\approx \Sigma_{BA} \chi_{-\sigma_A} = \sum_{i=1}^{N_i N-1} \int d\mathbf{r}_i V(\mathbf{r}_i - \mathbf{r}) [\chi_{+\sigma_B}(\mathbf{r}_i) \cdot \chi_{+\sigma_A}^*(\mathbf{r}_i)] \chi_{-\sigma_A}(\mathbf{r}) \\ &= \frac{1}{2^{3/2}} \sum_{i=1}^{N_i N-1} \int d\mathbf{r}_i V(\mathbf{r}_i - \mathbf{r}) \begin{bmatrix} e^{i\theta_{k_B}} \phi_2(\mathbf{r}_i) (-1) e^{-i\theta_{k_A}} \phi_2^*(\mathbf{r}_i) & e^{i\theta_{k_B}} \phi_2(\mathbf{r}_i) e^{-i\theta_{k_A}} \phi_1^*(\mathbf{r}_i) \\ e^{i\theta_{k_B}} \phi_1(\mathbf{r}_i) (-1) e^{-i\theta_{k_A}} \phi_2^*(\mathbf{r}_i) & e^{i\theta_{k_B}} \phi_1(\mathbf{r}_i) e^{-i\theta_{k_A}} \phi_1^*(\mathbf{r}_i) \end{bmatrix} \begin{bmatrix} e^{-i[(K_A - q_A)\mathbf{r} + \theta_{k_A}]} \phi_1(\mathbf{r}) \\ e^{-i[(K_A - q_A)\mathbf{r} + \theta_{k_A}]} \phi_2(\mathbf{r}) \end{bmatrix}. \end{aligned} \quad (19)$$

It follows from the expressions (18), (19) that the matrices Σ_{AB} and Σ_{BA} have the form

$$\Sigma_{AB} = \frac{1}{2} e^{\{-i(\theta_{k_A} - \theta_{k_B})\}} \sum_{i=1}^{N_i N-1} \int d\mathbf{r}_i V(\mathbf{r}_i - \mathbf{r}) \begin{bmatrix} \phi_1(\mathbf{r}_i) \phi_1^*(\mathbf{r}_i) & \phi_1(\mathbf{r}_i) \phi_2^*(\mathbf{r}_i) \\ \phi_2(\mathbf{r}_i) \phi_1^*(\mathbf{r}_i) & \phi_2(\mathbf{r}_i) \phi_2^*(\mathbf{r}_i) \end{bmatrix}, \quad (20)$$

$$\Sigma_{BA} = \frac{1}{2} e^{\{-i(\theta_{k_A} - \theta_{k_B})\}} \sum_{i=1}^{N_i N-1} \int d\mathbf{r}_i V(\mathbf{r}_i - \mathbf{r}) \begin{bmatrix} \phi_2(\mathbf{r}_i) \phi_2^*(\mathbf{r}_i) & -\phi_2(\mathbf{r}_i) \phi_1^*(\mathbf{r}_i) \\ -\phi_1(\mathbf{r}_i) \phi_2^*(\mathbf{r}_i) & \phi_1(\mathbf{r}_i) \phi_1^*(\mathbf{r}_i) \end{bmatrix}. \quad (21)$$

Let us find the matrices Σ_{AB} and Σ_{BA} in tight-binding approximation. To do it, we substitute the expression (16) into matrices (20), (21) and calculate integrals entered in elements of these matrices, for example

$$\int V(\mathbf{r}_i - \mathbf{r}) \phi_2(\mathbf{r}_i) \phi_1^*(\mathbf{r}_i) d\mathbf{r}_i = \frac{2}{(2\pi)^3 N} \int V(\mathbf{r}_i - \mathbf{r}) d\mathbf{r}_i \sum_{l_A', l_A} e^{i[K_A^i - q_A^i][\mathbf{R}_{l_A'} - \mathbf{R}_{l_A}]} \psi_{\{n_1\}}^*(\mathbf{r}_i - \mathbf{R}_{l_A'}) \psi_{\{n_2\}}(\mathbf{r}_i - \mathbf{R}_{l_A}). \quad (22)$$

Taking into account that the vector difference $\mathbf{r}_i - \mathbf{r}$ lays in i -th primitive cell: $\mathbf{r}_i - \mathbf{r} = \mathbf{r}_i^{2D}$, we transform (22) as

$$\begin{aligned} &\int V(\mathbf{r}_i - \mathbf{r}) \phi_2(\mathbf{r}_i) \phi_1^*(\mathbf{r}_i) d\mathbf{r}_i \\ &= \frac{2}{(2\pi)^3 N} \int V(\mathbf{r}_i^{2D}) d\mathbf{r}_i^{2D} \sum_{l_A', l_A} \exp\{i[\mathbf{K}_A^i - \mathbf{q}_A^i] \cdot [\tilde{\mathbf{R}}_{l_A'} - \tilde{\mathbf{R}}_{l_A}]\} \psi_{\{n_1\}}^*(\mathbf{r}_i^{2D} - \tilde{\mathbf{R}}_{l_A'}) \psi_{\{n_2\}}(\mathbf{r}_i^{2D} - \tilde{\mathbf{R}}_{l_A}) \end{aligned} \quad (23)$$

where i -th primitive cell is obtained from the base one by a rotation on an angle $(2i \pm 1)60^\circ$, $i=1, 2, 3$; $\tilde{\mathbf{R}}_{l_A(A')} = \mathbf{R}_{l_A(A')} - \mathbf{r}$. Let us account for nearest neighbors only in (23):

$$\int V(\mathbf{r}_i - \mathbf{r}) \phi_2(\mathbf{r}_i) \phi_1^*(\mathbf{r}_i) d\mathbf{r}_i = \frac{1}{(2\pi)^3} \exp\{i[\mathbf{K}_A^i - \mathbf{q}_A^i] \cdot \boldsymbol{\delta}_i\} \int V(\mathbf{r}_i^{2D}) \psi_{\{n_1\}}^*(\mathbf{r}_i^{2D} - \boldsymbol{\delta}_i) \psi_{\{n_2\}}(\mathbf{r}_i^{2D}) d\mathbf{r}_i^{2D}. \quad (24)$$

As a basic set we choose $\psi_{\{n_2\}}, \psi_{\{n_1\}}$ orbitals of π -electrons: $\psi_{\{n_2\}} = c_1 \psi_{p_z}(\mathbf{r} \pm \boldsymbol{\delta}_i) + c_2 \psi_{p_z}(\mathbf{r})$, $\sum_{i=1}^2 c_i^2 = 1$; $\psi_{\{n_1\}} = \psi_{p_z}(\mathbf{r})$. Energy of an electron is not changed with rotation on a lattice vector. Therefore, we can use the symmetry of the problem for simulation simplification by choosing e.g., $\boldsymbol{\delta}_i$ and \mathbf{q} , as $\boldsymbol{\delta}_i$, \mathbf{q}_i .

4. Partially Broken Symmetry of Model $N = 3$

Substituting the expression (23) into the matrixes (20), (21) and choosing basic set with $c_1 = c_2 = 1/\sqrt{2}$, we get in the approximation (24):

$$\begin{aligned} \Sigma_{AB}(\delta_i q_i) &= \frac{1}{\sqrt{2}(2\pi)^3} e^{-i(\theta_{k_A} - \theta_{k_B})} \sum_{i=1}^3 \exp\{i[\mathbf{K}_A^i - \mathbf{q}_i] \cdot \boldsymbol{\delta}_i\} \int dz \int V(\mathbf{r}_{2D}) dx_{2D} dy_{2D} \\ &\times \left(\begin{array}{cc} \sqrt{2} \psi_{p_z}(\mathbf{r}_{2D}) \psi_{p_z, -\boldsymbol{\delta}_i}^*(\mathbf{r}_{2D}) & \psi_{p_z}(\mathbf{r}_{2D}) [\psi_{p_z}^*(\mathbf{r}_{2D}) + \psi_{p_z, -\boldsymbol{\delta}_i}^*(\mathbf{r}_{2D})] \\ \psi_{p_z, -\boldsymbol{\delta}_i}^*(\mathbf{r}_{2D}) [\psi_{p_z, \boldsymbol{\delta}_i}(\mathbf{r}_{2D}) + \psi_{p_z}(\mathbf{r}_{2D})] & [\psi_{p_z, \boldsymbol{\delta}_i}(\mathbf{r}_{2D}) + \psi_{p_z}(\mathbf{r}_{2D})] [\psi_{p_z}^*(\mathbf{r}_{2D}) + \psi_{p_z, -\boldsymbol{\delta}_i}^*(\mathbf{r}_{2D})] / \sqrt{2} \end{array} \right) \\ &= \frac{1}{\sqrt{2}(2\pi)^3} e^{-i(\theta_{k_A} - \theta_{k_B})} \sum_{i=1}^3 \exp\{i[\mathbf{K}_A^i - \mathbf{q}_i] \cdot \boldsymbol{\delta}_i\} \Sigma_{AB}^{nd}, \end{aligned} \quad (25)$$

$$\begin{aligned} \Sigma_{BA}(\delta_i q_i) &= \frac{1}{\sqrt{2}(2\pi)^3} e^{-i(\theta_{k_A} - \theta_{k_B})} \sum_{i=1}^3 \exp\{i[\mathbf{K}_A^i - \mathbf{q}_i] \cdot \boldsymbol{\delta}_i\} \int dz \int V(\mathbf{r}_{2D}) dx_{2D} dy_{2D} \\ &\times \left(\begin{array}{cc} \frac{1}{\sqrt{2}} [\psi_{p_z, \boldsymbol{\delta}_i}(\mathbf{r}_{2D}) + \psi_{p_z}(\mathbf{r}_{2D})] [\psi_{p_z}^*(\mathbf{r}_{2D}) + \psi_{p_z, -\boldsymbol{\delta}_i}^*(\mathbf{r}_{2D})] & -\psi_{p_z, -\boldsymbol{\delta}_i}^*(\mathbf{r}_{2D}) [\psi_{p_z, \boldsymbol{\delta}_i}(\mathbf{r}_{2D}) + \psi_{p_z}(\mathbf{r}_{2D})] \\ -\psi_{p_z}(\mathbf{r}_{2D}) [\psi_{p_z}^*(\mathbf{r}_{2D}) + \psi_{p_z, -\boldsymbol{\delta}_i}^*(\mathbf{r}_{2D})] & \sqrt{2} \psi_{p_z}(\mathbf{r}_{2D}) \psi_{p_z, -\boldsymbol{\delta}_i}^*(\mathbf{r}_{2D}) \end{array} \right) \\ &= \frac{1}{\sqrt{2}(2\pi)^3} e^{-i(\theta_{k_A} - \theta_{k_B})} \sum_{i=1}^3 \exp\{i[\mathbf{K}_A^i - \mathbf{q}_i] \cdot \boldsymbol{\delta}_i\} \Sigma_{BA}^{nd}. \end{aligned} \quad (26)$$

Here it was chosen the upper sign for π -orbital $\psi_{\{n_2\}}$ and was introduced the following notion $\psi_{p_z, \pm \boldsymbol{\delta}_i}(\mathbf{r}_{2D}) = \psi_{p_z}(\mathbf{r}_{2D} \pm \boldsymbol{\delta}_i)$. Secular equation with this basic orthogonal set $\{|i\rangle\}$ has the form

$$\langle i | \boldsymbol{\sigma}_{2D}^{BA} \cdot \mathbf{p}_{AB} | \psi \rangle = \sum_j \langle i | \hat{v}_F^{-1} | j \rangle \langle j | E | \psi \rangle = \frac{1}{\langle i | \hat{v}_F | i \rangle} \langle i | E | \psi \rangle. \quad (27)$$

Due to the fact that $\langle i | \hat{v}_F | i \rangle \propto v_F$ and the wave function is defined up to a phase multiplier, then Equation (27) is reduced to

$$\boldsymbol{\sigma}_{2D}^{BA} \cdot \mathbf{p}_{AB} | \chi \rangle = \frac{E}{v_F} | \chi \rangle. \quad (28)$$

Let us rewrite Equation (28) in momentum representation as

$$\sum_{i,j} \langle \chi_p | q_i \rangle \Sigma_{AB}(\delta_i q_i) \boldsymbol{\sigma}_{2D} \Sigma_{AB}^{-1}(\delta_j q_j) \langle q_j | \mathbf{p}_{AB} | \chi_p \rangle = \langle \chi_p | \frac{E_p}{v_F} | \chi_p \rangle \quad (29)$$

where $\mathbf{q}_i + \mathbf{q}_j = 0$ owing to momentum conservation law. Then one can obtain $\boldsymbol{\sigma}_{2D}^{BA}$ in an explicit form

$$\boldsymbol{\sigma}_{2D}^{BA} \equiv \Sigma_{AB}(\delta_i q_i) \boldsymbol{\sigma}_{2D} \Sigma_{AB}^{-1}(\delta_j q_j) = -\Sigma_{AB}^{nd} \boldsymbol{\sigma}_{2D} (\Sigma_{AB}^{nd})^{-1} \frac{\sum_{k=1}^3 [1 - i(\mathbf{q} \cdot \boldsymbol{\delta}_k) - (\mathbf{q} \cdot \boldsymbol{\delta}_k)^2 - \dots]}{\sum_{k=1}^3 [1 + i(\mathbf{q} \cdot \boldsymbol{\delta}_k) - (\mathbf{q} \cdot \boldsymbol{\delta}_k)^2 + \dots]}. \quad (30)$$

Substituting known expressions for eigenfunctions of hydrogen-like atom [47] and evaluating integrals, we obtain rather lengthy (\mathbf{q})-dependent invertible matrices, for $\mathbf{q} = 0$ they are pure numeric and up to a common scalar prefactor read

$$\Sigma_{AB}(\mathbf{K}_A) = \begin{pmatrix} 0.062 & 0.54 \\ 0.045 & 0.42 \end{pmatrix}, \quad \Sigma_{BA}(\mathbf{K}_A) = \begin{pmatrix} 0.42 & -0.045 \\ -0.54 & 0.062 \end{pmatrix}. \quad (31)$$

The most interesting thing is that eigenvalue problem (28) gives precisely the known dispersion laws $E(\mathbf{q}) = \pm \sqrt{q_x^2 + q_y^2}$, that is problem is persistent up to $|q|^3$ variations.

Now, we take into account higher order in $|q|$ terms when evaluating Σ_{AB}, Σ_{BA} . Dependence of the Fermi energy $E_F(n)$ on the surface carriers concentration n is the replacement of

$E(|q|/|K_A|) \rightarrow E_F(|q|/k_F) = E_F(|q|/\sqrt{\pi n})$ so that $q_x^2 + q_y^2 = \pi n = k_F^2$. The Fermi energies $E_F^e(n)$ and

$E_F^h(n)$ for electrons and holes, respectively, are represented in **Figure 1**. One can see that the hole and electron bands are symmetric. Six mini-zones around points K, K' of Brillouin zone are also observable in **Figure 1**.

5. Asymmetrical Charged Carriers at Large Fermion Density

Now, let us show that the spectrum $E(\mathbf{q})$ corresponding to Equation (12) can deviate from the conic form at large concentration n . According to **Figure 1**, for $n \sim 10^{14} \text{ m}^{-2}$ the Fermi level is in the region with unbroken symmetry of the Dirac cone. When $n \sim 10^{15} \text{ m}^{-2}$, the Fermi level enters the region with broken symmetry of the Dirac cone. In this region, there is a Fermi energy curve $E_F^{e(h)}$ which has local hyperbolic points of a “saddle” type. Fermi curves passing through or near these hyperbolic points are local maxima and minima. Since in these points “trajectories” of quasi-particle motion (*i.e.*, the configuration space of the system) are unstable, not all holes (electrons) can reach the Dirac cone (replicas) and annihilate. We demonstrate $E(\mathbf{q})$ surface sections for few q_x in **Figure 2**.

Figure 2(a) emphasizes that in the vicinity of Dirac point the cone is persistent due to symmetry (section crosses original cone and its replicas simultaneously), at higher values of q , higher order corrections start to contribute. An energy dispersion law for 2D graphene is linear near Dirac cone corner at $\mu = 0$ (see **Figure 2(a)**). When section crosses original cone only (**Figure 2(b)**), we find symmetrical section of the Dirac cone.

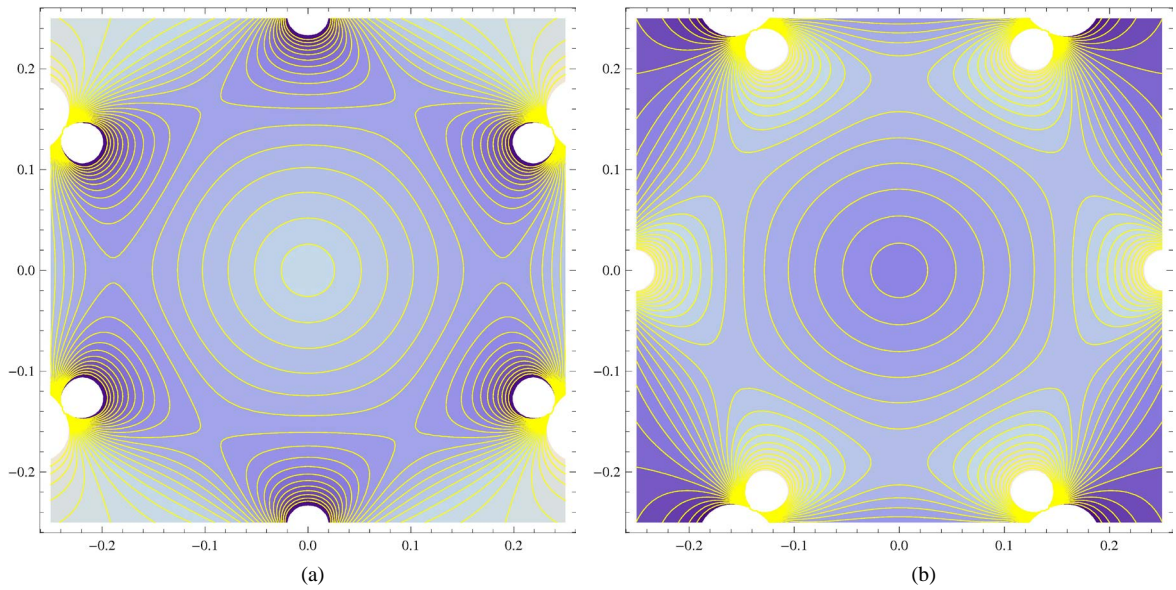


Figure 1. Fermi energy $E_F(n)$ curves at different carrier concentrations n for electrons (a) and holes (b).

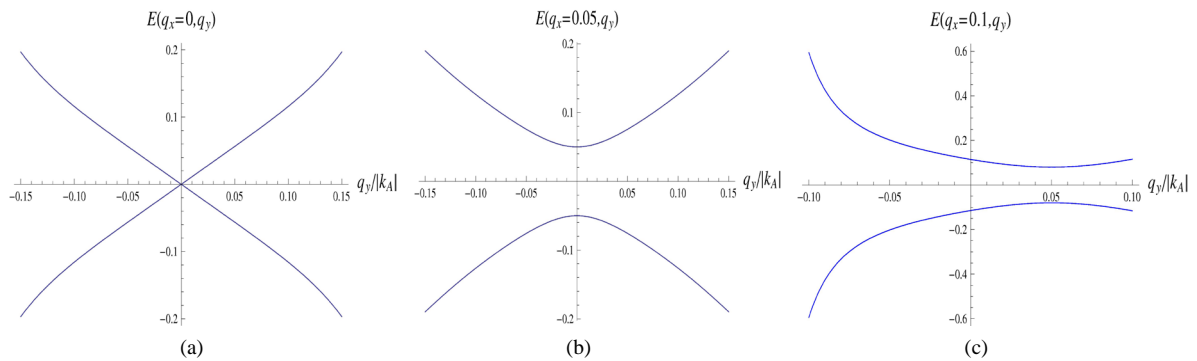


Figure 2. The dependence $E(q_x, q_y)$ for several different values of q_x : (a) $q_x/|K_A| = 0$; (b) $q_x/|K_A| = 0.05$; (c) $q_x/|K_A| = 0.1$.

Comparing **Figure 2(c)** with **Figure 1** we can conclude that the section of Dirac cone and its replicas at $q_x/|K_A|=0.1$ is placed in one of six mini-zones of the Brillouin zone. It leads to electron-hole asymmetry. Such type of charged carrier asymmetry has been observed in [32] [33] as the resistivity dependence upon direct current at positive and negative values of the gate voltage. We can compare an energy distance between “upper” and “lower” Dirac cones with an energy distance between replicas in section given by the relation $q_x/|K_A|=0.1$. In such a section the extremum takes place at $q_y/|K_A|=0.05$ (**Figure 2(c)**). The distance ΔE_R between extrema at $q_y/|K_A|=0.05$ is the distance between nearest upper and lower replicas. $\Delta E_R \approx 0.02K_A v_F$, due to rotation of Dirac cone in respect to replicas at $q \neq 0$.

Thus, the six fold rotational symmetry of graphene energy surface near the Dirac point partially breaks, except of Dirac cone’s corner, and, respectively the Dirac cone does not coincide with its replicas.

6. Electron-Hole Localization in the Model $N = 3$ at Low Carrier Concentration

The displacement of replicas points in the graphene Brillouin zone on respect to the primary Dirac cone points occurs at a distance

$$|\Delta \mathbf{q}_{AB}| = |\mathbf{q}_{AB} - \mathbf{q}_{BA}|. \quad (32)$$

Since in the neighborhood of the Dirac cone’s corner $q \rightarrow 0$, and (as was shown above) the cone persists then, in accord with (32) in the graphene Brillouin zone all points of the Dirac cone replicas shift, except of their corners. To understand what value of the rotation angle it could correspond to, we choose $\mathbf{k} \propto 0.1\mathbf{K}_A$ and find $\Delta \mathbf{k}_{AB}$ based on (32) and expressions (31) for Σ_{BA}, Σ_{AB} . The rotation angle $\arccos((\mathbf{w}_1 \cdot \mathbf{w}_2)/|\mathbf{w}_1||\mathbf{w}_2|) = 1.57076$ so it turns out to be a practically right angle $\pi/2$ where $\mathbf{w}_1 = \Sigma_{AB}\mathbf{k}\Sigma_{AB}^{-1}$, $\mathbf{w}_2 = \Sigma_{BA}\mathbf{k}\Sigma_{BA}^{-1}$. The last means that the rotation could be large enough for some points in momentum space.

Let us find localization regions of non-annihilated quasiparticles. Since momenta \mathbf{q}_h of holes are rotated with respect to the electron momenta \mathbf{q}_e at angle $\pi/2$, the hole Fermi curve E_F^h is also rotated. Because of the symmetry, the curve E_F^h is effectively rotated at angle $\pi/6$, as shown in **Figure 1**. Adding E_F^e and the corresponding to it a hole Fermi surface $-E_F^h$, we find the surface $S(n) \equiv E_F^e - E_F^h$, which demonstrates charge density distribution at the Fermi level $\mu \rightarrow 0$ at low charged carriers concentrations $n \ll 1$ and is shown in **Figure 3**. $S(n)$ takes nonzero values outside of Dirac cone’s corner (non-zero values of the chemical potential μ).

By virtue of turn of the holes valence band (conduction band electrons) at $\pi/6$, the hole liquid is localized so that the electron liquid from its valence band could flow into the vacancies of the hole valence band. Similarly,

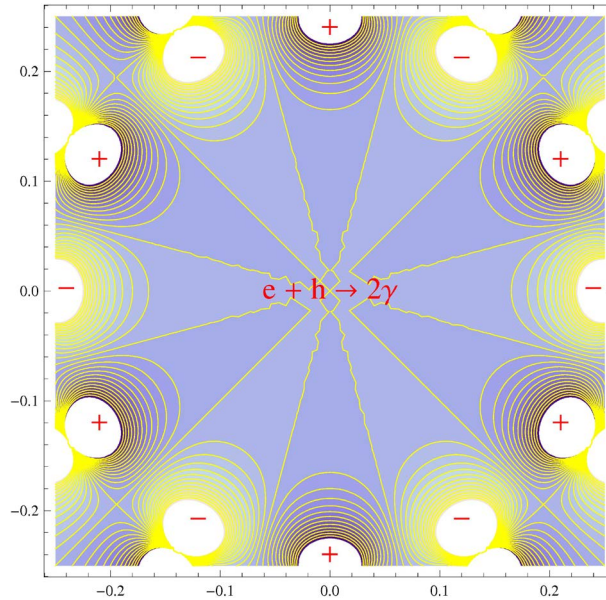


Figure 3. Scheme of localization in flavor model $N = 3$.

the hole liquid flows into the vacancies of the valence band electrons at some value $\mu = \pm\delta, \delta \ll 1$. Since the annihilation processes are absent, the hole and electron Fermi levels are not at $\mu = 0$, and stabilized at some value $\mu = \pm\delta$ and, respectively, the Fermi level is dynamic. Therefore, there is a dynamic overlapping of valence and conduction bands, and, respectively, clear graphene turns out to be a metal. The neighborhood with $\mu \rightarrow 0$ is a region where trapped quasiparticles could annihilate; therefore the charged carriers there, are practically absent. This actually is the prohibition for charge carriers to be in the Dirac cone's corner.

The formed dynamic equilibrium can be disturbed by injection of carriers δn from outside into a forbidden neighborhood $\mu \rightarrow 0$. Then, to restore the balance, the charge carriers will move into the forbidden region with subsequent annihilation $e + h \rightarrow 2\gamma$ and, consequently, having opposite sign free carriers appears in the regions of localization. The energy δE of the free carriers is equal to energy of both quanta: $\delta E \sim 2\hbar\omega_\gamma\delta n$. Since δn is small, the "sea" of free quasiparticles is a shallow one. According to **Figure 3**, due to hyperbolic points, between basins of electrons and holes there are unstable regions, which leads to disintegration of the large "see" into separate small "puddles". Such "puddles" are experimentally observed at $\delta n < 10^{15} \text{ m}^{-2}$ [48].

7. Conclusion

The physical flavors approach $N = 3$ to a quantum field description of graphene electronic properties has been developed. It is based on the Dirac-Hartree-Fock self-consistent field approximation and assumption on antiferromagnetic ordering of graphene lattice. The approach is a generalization of the known model $N = 2$ of massless Dirac fermions in graphene. Its first advantage is that the model $N = 3$ gives symmetric electron and hole band structures, which differ from the band structure model $N = 2$ only by a partial violation of the order of $|q|^4$ of the six-fold rotational symmetry of primary Dirac cone and its replicas. In the cone's corner $|q| \rightarrow 0$ the Dirac cone is degenerated. The second advantage is the possibility to account for charged carriers asymmetry stipulated by exchange interaction potential for different sublattices. The third flavor, given by transformations Σ_{AB}, Σ_{BA} , gives charged carriers asymmetry and is expressed in dynamical location of the Fermi level and dynamical localization of electrons and holes.

References

- [1] Grushevskaya, G.V., Komarov, L.I. and Gurskii, L.I. (1998) *Physics of Solid State*, **40**, 1802-1805. <http://dx.doi.org/10.1134/1.1130660>
- [2] Gusynin, V.P., Sharapov, S.G. and Carbotte, J.P. (2007) *International Journal of Modern Physics B*, **21**, 4611. <http://dx.doi.org/10.1142/S0217979207038022>
- [3] Peres, N.M.R. (2009) *Journal of Physics: Condensed Matter*, **21**, 323201. <http://dx.doi.org/10.1088/0953-8984/21/32/323201>
- [4] Ziegler, K. (2007) *Physical Review B*, **75**, 233407. <http://dx.doi.org/10.1103/PhysRevB.75.233407>
- [5] Ando, T., Zheng, Y. and Suzuura, H. (2002) *Journal of the Physical Society of Japan*, **71**, 1318-1324. <http://dx.doi.org/10.1143/JPSJ.71.1318>
- [6] Novoselov, K.S., Geim, A.K., Morozov, S.V., et al. (2004) *Science*, **306**, 666. <http://dx.doi.org/10.1143/JPSJ.71.1318>
- [7] Dean, C.R., Young, A.F. and Meric, I. (2010) *Nature Nanotechnology*, **5**, 722. <http://dx.doi.org/10.1038/nnano.2010.172>
- [8] Bolotin, K.I., Sikes, K.J., Hone, J., Stormer, H.L. and Kim, P. (2008) *Physical Review Letters*, **101**, 096802. <http://dx.doi.org/10.1103/PhysRevLett.101.096802>
- [9] Du, X., Skachko, I., Barker, A. and Andrei, E.Y. (2008) *Nature Nanotechnology*, **3**, 491-495. <http://dx.doi.org/10.1038/nnano.2008.199>
- [10] Geim, A.K. and Novoselov, K.S. (2007) *Nature Materials*, **6**, 183. <http://dx.doi.org/10.1038/nmat1849>
- [11] Castro, E.V., Ochoa, H., Katsnelson, M.I., Gorbachev, R.V., Elias, D.C., Novoselov, K.S., Geim, A.K. and Guinea, F. (2010) *Physical Review Letters*, **105**, 266601. <http://dx.doi.org/10.1103/PhysRevLett.105.266601>
- [12] Hancock, Y. (2011) *Journal of Physics D*, **44**, 473001. <http://dx.doi.org/10.1088/0022-3727/44/47/473001>
- [13] Kibis, O.V. (2011) *Physical Review Letters*, **107**, 106802. <http://dx.doi.org/10.1103/PhysRevLett.107.106802>
- [14] Elias, D.C., Gorbachev, R.V., Mayorov, A.S., Morozov, S.V., Zhukov, A.A., Blake, P., Ponomarenko, L.A., Grigorieva, I.V., Novoselov, K.S., Guinea, F. and Geim, A.K. (2012) *Nature Physics*, **8**, 172. <http://dx.doi.org/10.1038/nphys2213>

- [15] Rojas-Cuervo, A.M. and Rey-González, R.R. (2013) Asymmetric Dirac Cones in Monatomic Hexagonal Lattices. ArXiv:1304.4576v1 [cond-mat.mes-hall]
- [16] Wang, J.R. and Liu, G.Z. (2011) *Journal of Physics: Condensed Matter*, **23**, 155602. <http://dx.doi.org/10.1088/0953-8984/23/15/155602>
- [17] Semenoff, G.W. (1984) *Physical Review Letters*, **53**, 2449. <http://dx.doi.org/10.1103/PhysRevLett.53.2449>
- [18] Wallace, P.R. (1947) *Physical Review*, **71**, 622-634. <http://dx.doi.org/10.1103/PhysRev.71.622>
- [19] Reich, S., Maultzsch, J., Thomsen, C. and Ordejón, P. (2002) *Physical Review B*, **66**, 035412. <http://dx.doi.org/10.1103/PhysRevB.66.035412>
- [20] Novoselov, K.S., Geim, A.K., Morozov, S.V., Jiang, D., Zhang, Y., Katsnelson, M.I., Grigorieva, I.V., Dubonos, S.V. and Firsov, A.A. (2005) *Nature*, **438**, 197-200. <http://dx.doi.org/10.1038/nature04233>
- [21] Fialkovsky, I. and Vassilevich, D.V. (2012) *European Physical Journal B*, **85**, 384. <http://dx.doi.org/10.1140/epjb/e2012-30685-9>
- [22] Falkovsky, L.A. (2011) *Low Temperature Physics*, **37**, 480-484. <http://dx.doi.org/10.1063/1.3615524>
- [23] Falkovsky, L.A. and Varlamov, A.A. (2007) *European Physical Journal B*, **56**, 281-284. <http://dx.doi.org/10.1140/epjb/e2007-00142-3>
- [24] Falkovsky, L.A. (2008) *Physics—Uspekhi*, **51**, 887-897. <http://dx.doi.org/10.1070/PU2008v051n09ABEH006625>
- [25] Gribov, V.N. (2001) Quantum Electrodynamics. Regular and Chaotic Dynamics Publisher, Izhevsk.
- [26] Kaku, M. (1994) Quantum Field Theory: A Modern Introduction. Oxford University Press, Oxford.
- [27] Abrikosov, A.A. (1998) *Physical Review B*, **58**, 2788. <http://dx.doi.org/10.1103/PhysRevB.58.2788>
- [28] Katsnelson, M.I. (2006) *European Physical Journal B*, **51**, 157-160. <http://dx.doi.org/10.1140/epjb/e2006-00203-1>
- [29] Kane, C.L. and Mele, E.J. (2005) *Physical Review Letters*, **95**, 226801. <http://dx.doi.org/10.1103/PhysRevLett.95.226801>
- [30] Huertas-Hernando, D., Guinea, F. and Brataas, A. (2006) *Physical Review B*, **74**, 155426. <http://dx.doi.org/10.1103/PhysRevB.74.155426>
- [31] Min, H., Hill, J.E., Sinitsyn, N.A., Sahu, B.R., Kleinman, L. and MacDonald, A.H. (2006) *Physical Review B*, **74**, 165310. <http://dx.doi.org/10.1103/PhysRevB.74.165310>
- [32] Han, W., McCreary, K., Bao, W., Li, Y., Miao, F., Lau, C.N. and Kawakami, R.K. (2009) *Physical Review Letters*, **102**, 137205. <http://dx.doi.org/10.1103/PhysRevLett.102.137205>
- [33] Han, W., McCreary, K., Pi, K., Wang, W.H., Li, Y., Wen, H., Chen, J.R. and Kawakami, R.K. (2012) *Journal of Magnetism and Magnetic Materials*, **324**, 369-381. <http://dx.doi.org/10.1016/j.jmmm.2011.08.001>
- [34] Pesin, D. and MacDonald, A.H. (2012) *Nature Materials*, **11**, 409-416. <http://dx.doi.org/10.1038/nmat3305>
- [35] Elias, D.C., Gorbachev, R.V., Mayorov, A.S., Morozov, S.V., Zhukov, A.A., Blake, P., Ponomarenko, L.A., Grigorieva, I.V., Novoselov, K.S., Guinea, F. and Geim, A.K. (2011) *Nature Physics*, **7**, 701-704. <http://dx.doi.org/10.1038/nphys2049>
- [36] Ferreira, A., Rappoport, T.G., Casalilla, M.A. and Neto, A.H.C. (2014) *Physical Review Letters*, **112**, 066601. <http://dx.doi.org/10.1103/PhysRevLett.112.066601>
- [37] Neto, A.H.C., Guinea, F., Peres, N.M., Novoselov, K.S. and Geim, A.K. (2009) *Reviews of Modern Physics*, **81**, 109-162. <http://dx.doi.org/10.1103/RevModPhys.81.109>
- [38] Dirac, P.A.M. (1966) Lectures on Quantum Field Theory. Belfer Graduate School of Science, New York.
- [39] Grushevskaya, H.V. and Krylov, G.G. (2013) *Int. J. Nonlin. Phen. in Comp. Sys.*, **16**, 189-208.
- [40] Rahman, A., Guikema, J.W. and Marković, N. (2013) Asymmetric Scattering of Dirac Electrons and Holes in Graphene. arXiv:1304.6318v1 [cond-mat.mes-hall]
- [41] Rahman, A., Guikema, J.W. and Marković, N. (2013) Direct Evidence of Angle-Selective Transmission of Dirac Electrons in Graphene p-n Junctions. arXiv:1304.5533v1 [cond-mat.mes-hall]
- [42] Rossi, E., Bardarson, J.H., Fuhrer, M.S. and Das, S.S. (2012) *Physical Review Letters*, **109**, 096801. <http://dx.doi.org/10.1103/PhysRevLett.109.096801>
- [43] Grushevskaya, H.V. and Krylov, G.G. (2014) *Int. J. Nonlin. Phen. in Comp. Sys.*, **17**, 86-96.
- [44] Grushevskaya, H.V. and Krylov, G.G. (2013) Electronic Structure and Transport in Graphene: Quasi-Relativistic Dirac-Hartree-Fock Self-Consistent Field Approximation. arXiv:1309.1847 [cond-mat.mes-hall]
- [45] Krylov, G.G., Krylova, H.V. and Belov, M.A. (2011) Electron Transport in Low-Dimensional Systems with Nontrivial

Topology: Effects of Localization. In: Mokshin, A.V., *et al.*, Eds., *Dynamical Phenomena in Complex Systems*, MOiN RT Publishing, Kazan, 161-180. (in Russian)

- [46] Krylova, H. and Hursky, L. (2013) Spin Polarization in Strong-Correlated Nanosystems. LAP LAMBERT Academic Publishing, Saarbrücken.
- [47] Messiah, A. (2000) Quantum Mechanics, Vol. 1. Dover Publications, Mineola.
- [48] Morozov, S.V., Novoselov, K.S. and Geim, A.K. (2008) *Physics—Uspekhi*, **178**, 776.